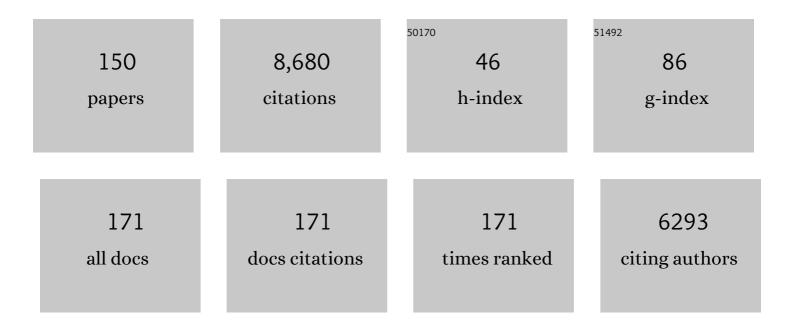
## Anja Böckmann

List of Publications by Year in descending order

Source: https://exaly.com/author-pdf/1509088/publications.pdf Version: 2024-02-01



ΔΝΙΑ ΒΑσκμανι

#	Article	IF	CITATIONS
1	Correction of field instabilities in biomolecular solid-state NMR by simultaneous acquisition of a frequency reference. Magnetic Resonance, 2022, 3, 15-26.	0.8	2
2	Fast Magicâ€Angle‧pinning NMR Reveals the Evasive Hepatitisâ€B Virus Capsid Câ€Terminal Domain**. Angewandte Chemie, 2022, 134, .	1.6	1
3	Fast Magicâ€Angle‧pinning NMR Reveals the Evasive Hepatitisâ€B Virus Capsid Câ€Terminal Domain**. Angewandte Chemie - International Edition, 2022, 61, .	7.2	9
4	Pharmacomodulation of a ligand targeting the HBV capsid hydrophobic pocket. Chemical Science, 2022, 13, 8840-8847.	3.7	1
5	Solid-State NMR Reveals Asymmetric ATP Hydrolysis in the Multidrug ABC Transporter BmrA. Journal of the American Chemical Society, 2022, 144, 12431-12442.	6.6	13
6	Dimer Organization of Membraneâ€Associated NS5A of Hepatitisâ€C Virus as Determined by Highly Sensitive 1 Hâ€Detected Solidâ€State NMR. Angewandte Chemie, 2021, 133, 5399-5407.	1.6	3
7	Dimer Organization of Membraneâ€Associated NS5A of Hepatitisâ€C Virus as Determined by Highly Sensitive <sup>1</sup> Hâ€Detected Solidâ€State NMR. Angewandte Chemie - International Edition, 2021, 60, 5339-5347.	7.2	25
8	Easy Synthesis of Complex Biomolecular Assemblies: Wheat Germ Cell-Free Protein Expression in Structural Biology. Frontiers in Molecular Biosciences, 2021, 8, 639587.	1.6	21
9	A pocket-factor–triggered conformational switch in the hepatitis B virus capsid. Proceedings of the National Academy of Sciences of the United States of America, 2021, 118, e2022464118.	3.3	15
10	Large-Scale Recombinant Production of the SARS-CoV-2 Proteome for High-Throughput and Structural Biology Applications. Frontiers in Molecular Biosciences, 2021, 8, 653148.	1.6	29
11	Paramagnetic Solidâ€State NMR to Localize the Metalâ€Ion Cofactor in an Oligomeric DnaB Helicase. Chemistry - A European Journal, 2021, 27, 7745-7755.	1.7	8
12	Temperature-Dependent Solid-State NMR Proton Chemical-Shift Values and Hydrogen Bonding. Journal of Physical Chemistry B, 2021, 125, 6222-6230.	1.2	13
13	Biomolecular solid-state NMR spectroscopy at 1200ÂMHz: the gain in resolution. Journal of Biomolecular NMR, 2021, 75, 255-272.	1.6	41
14	A fusion peptide in preS1 and the human protein disulfide isomerase ERp57 are involved in hepatitis B virus membrane fusion process. ELife, 2021, 10, .	2.8	12
15	Spectroscopic glimpses of the transition state of ATP hydrolysis trapped in a bacterial DnaB helicase. Nature Communications, 2021, 12, 5293.	5.8	13
16	Hommage to Richard R. Ernst. Frontiers in Molecular Biosciences, 2021, 8, 769772.	1.6	0
17	Experimental Characterization of the Hepatitis B Virus Capsid Dynamics by Solid-State NMR. Frontiers in Molecular Biosciences, 2021, 8, 807577.	1.6	9
18	Phosphorylation of the Hepatitis B Virus Large Envelope Protein. Frontiers in Molecular Biosciences, 2021, 8, 821755.	1.6	1

#	Article	IF	CITATIONS
19	Nucleotide Binding Modes in a Motor Protein Revealed by <sup>31</sup> P―and <sup>1</sup> Hâ€Detected MAS Solidâ€State NMR Spectroscopy. ChemBioChem, 2020, 21, 324-330.	1.3	20
20	Protonâ€Detected Solidâ€State NMR of the Cellâ€Free Synthesized αâ€Helical Transmembrane Protein NS4B from Hepatitis C Virus. ChemBioChem, 2020, 21, 1453-1460.	1.3	16
21	Solid-State NMR for Studying the Structure and Dynamics of Viral Assemblies. Viruses, 2020, 12, 1069.	1.5	29
22	ATP Analogues for Structural Investigations: Case Studies of a DnaB Helicase and an ABC Transporter. Molecules, 2020, 25, 5268.	1.7	27
23	In vitro translation of virally-encoded replication polyproteins to recapitulate polyprotein maturation processes. Protein Expression and Purification, 2020, 175, 105694.	0.6	3
24	Asparagine and Glutamine Side-Chains and Ladders in HET-s(218–289) Amyloid Fibrils Studied by Fast Magic-Angle Spinning NMR. Frontiers in Molecular Biosciences, 2020, 7, 582033.	1.6	12
25	Prion Amyloid Polymorphs – The Tag Might Change It All. Frontiers in Molecular Biosciences, 2020, 7, 190.	1.6	2
26	Protein NMR Spectroscopy at 150â€kHz Magicâ€Angle Spinning Continues To Improve Resolution and Mass Sensitivity. ChemBioChem, 2020, 21, 2540-2548.	1.3	72
27	Sedimentation Yields Long-Term Stable Protein Samples as Shown by Solid-State NMR. Frontiers in Molecular Biosciences, 2020, 7, 17.	1.6	32
28	Quantifying proton NMR coherent linewidth in proteins under fast MAS conditions: a second moment approach. Physical Chemistry Chemical Physics, 2019, 21, 18850-18865.	1.3	33
29	100 kHz MAS Proton-Detected NMR Spectroscopy of Hepatitis B Virus Capsids. Frontiers in Molecular Biosciences, 2019, 6, 58.	1.6	38
30	Including Protons in Solid-State NMR Resonance Assignment and Secondary Structure Analysis: The Example of RNA Polymerase II Subunits Rpo4/7. Frontiers in Molecular Biosciences, 2019, 6, 100.	1.6	14
31	Combining Cell-Free Protein Synthesis and NMR Into a Tool to Study Capsid Assembly Modulation. Frontiers in Molecular Biosciences, 2019, 6, 67.	1.6	20
32	Spinning faster: protein NMR at MAS frequencies up to 126ÂkHz. Journal of Biomolecular NMR, 2019, 73, 19-29.	1.6	101
33	Protein sample preparation for solid-state NMR investigations. Progress in Nuclear Magnetic Resonance Spectroscopy, 2019, 110, 20-33.	3.9	23
34	Flexible-to-rigid transition is central for substrate transport in the ABC transporter BmrA from Bacillus subtilis. Communications Biology, 2019, 2, 149.	2.0	32
35	Phosphorylation and Alternative Translation on Wheat Germ Cell-Free Protein Synthesis of the DHBV Large Envelope Protein. Frontiers in Molecular Biosciences, 2019, 6, 138.	1.6	7
36	A Substantial Structural Conversion of the Native Monomer Leads to inâ€Register Parallel Amyloid Fibril Formation in Lightâ€Chain Amyloidosis. ChemBioChem, 2019, 20, 1027-1031.	1.3	21

#	Article	IF	CITATIONS
37	The conformational changes coupling ATP hydrolysis and translocation in a bacterial DnaB helicase. Nature Communications, 2019, 10, 31.	5.8	45
38	Two new polymorphic structures of human full-length alpha-synuclein fibrils solved by cryo-electron microscopy. ELife, 2019, 8, .	2.8	220
39	Structural Studies of Self-Assembled Subviral Particles: Combining Cell-Free Expression with 110â€kHz MAS NMR Spectroscopy. Angewandte Chemie - International Edition, 2018, 57, 4787-4791.	7.2	37
40	Strukturelle Untersuchung subviraler Partikel durch die Kombination von zellfreier Proteinherstellung mit 110 kHz MAS-NMR-Spektroskopie. Angewandte Chemie, 2018, 130, 4877-4882.	1.6	4
41	Solid-state [13C–15N] NMR resonance assignment of hepatitis B virus core protein. Biomolecular NMR Assignments, 2018, 12, 205-214.	0.4	21
42	Localizing Conformational Hinges by NMR: Where Do Hepatitis B Virus Core Proteins Adapt for Capsid Assembly?. ChemPhysChem, 2018, 19, 1336-1340.	1.0	25
43	Binding of Polythiophenes to Amyloids: Structural Mapping of the Pharmacophore. ACS Chemical Neuroscience, 2018, 9, 475-481.	1.7	31
44	Selective labeling and unlabeling strategies in protein solid-state NMR spectroscopy. Journal of Biomolecular NMR, 2018, 71, 141-150.	1.6	49
45	CONFINE-MAS: a magic-angle spinning NMR probe that confines the sample in case of a rotor explosion. Journal of Biomolecular NMR, 2018, 72, 171-177.	1.6	5
46	Direct amide 15N to 13C transfers for solid-state assignment experiments in deuterated proteins. Journal of Biomolecular NMR, 2018, 72, 69-78.	1.6	4
47	High-spin Metal Centres in Dipolar EPR Spectroscopy. Chimia, 2018, 72, 216-220.	0.3	3
48	Amyloid Fibril Polymorphism: Almost Identical on the Atomic Level, Mesoscopically Very Different. Journal of Physical Chemistry B, 2017, 121, 1783-1792.	1.2	41
49	Line-Broadening in Low-Temperature Solid-State NMR Spectra of Fibrils. Journal of Biomolecular NMR, 2017, 67, 51-61.	1.6	26
50	Partially-deuterated samples of HET-s(218–289) fibrils: assignment and deuterium isotope effect. Journal of Biomolecular NMR, 2017, 67, 109-119.	1.6	30
51	Solidâ€state NMR and EPR Spectroscopy of Mn <sup>2+</sup> â€6ubstituted ATPâ€Fueled Protein Engines. Angewandte Chemie - International Edition, 2017, 56, 3369-3373.	7.2	49
52	Overall Structural Model of NS5A Protein from Hepatitis C Virus and Modulation by Mutations Confering Resistance of Virus Replication to Cyclosporin A. Biochemistry, 2017, 56, 3029-3048.	1.2	29
53	Hexagonal ice in pure water and biological NMR samples. Journal of Biomolecular NMR, 2017, 67, 15-22.	1.6	1
54	Emerging Structural Understanding of Amyloid Fibrils by Solid-State NMR. Trends in Biochemical Sciences, 2017, 42, 777-787.	3.7	73

#	Article	IF	CITATIONS
55	Proton-Detected NMR Spectroscopy of Nanodisc-Embedded Membrane Proteins: MAS Solid-State vs Solution-State Methods. Journal of Physical Chemistry B, 2017, 121, 7671-7680.	1.2	23
56	Sample Preparation for Membrane Protein Structural Studies by Solid-State NMR. Methods in Molecular Biology, 2017, 1635, 345-358.	0.4	5
57	Wheat Germ Cell-Free Overexpression for the Production of Membrane Proteins. Methods in Molecular Biology, 2017, 1635, 91-108.	0.4	17
58	Festkörperâ€NMR―und EPR‧pektroskopie an Mn <sup>2+</sup> â€substituierten ATPâ€angetriebenen Proteinmaschinen. Angewandte Chemie, 2017, 129, 3418-3422.	1.6	5
59	Protein–nucleotide contacts in motor proteins detected by DNP-enhanced solid-state NMR. Journal of Biomolecular NMR, 2017, 69, 157-164.	1.6	19
60	The conformation of the Congo-red ligand bound to amyloid fibrils HET-s(218–289): a solid-state NMR study. Journal of Biomolecular NMR, 2017, 69, 207-213.	1.6	8
61	Gradient reconstitution of membrane proteins for solid-state NMR studies. Journal of Biomolecular NMR, 2017, 69, 81-91.	1.6	11
62	An Efficient Procedure for Removal and Inactivation of Alpha-Synuclein Assemblies from Laboratory Materials. Journal of Parkinson's Disease, 2016, 6, 143-151.	1.5	31
63	Cell-free expression, purification, and membrane reconstitution for NMR studies of the nonstructural protein 4B from hepatitis C virus. Journal of Biomolecular NMR, 2016, 65, 87-98.	1.6	25
64	Further exploration of the conformational space of α-synuclein fibrils: solid-state NMR assignment of a high-pH polymorph. Biomolecular NMR Assignments, 2016, 10, 5-12.	0.4	36
65	Solid-state NMR sequential assignment of an Amyloid-β(1–42) fibril polymorph. Biomolecular NMR Assignments, 2016, 10, 269-276.	0.4	18
66	Variability and conservation of structural domains in divide-and-conquer approaches. Journal of Biomolecular NMR, 2016, 65, 79-86.	1.6	15
67	Atomic-resolution structure of a disease-relevant Aβ(1–42) amyloid fibril. Proceedings of the National Academy of Sciences of the United States of America, 2016, 113, E4976-84.	3.3	712
68	Beobachtung von ssDNAâ€Bindung an die DnaBâ€Helikase von <i>Helicobacter pylori</i> mittels Festkörperâ€NMRâ€5pektroskopie. Angewandte Chemie, 2016, 128, 14370-14375.	1.6	4
69	Monitoring ssDNA Binding to the DnaB Helicase from <i>Helicobacter pylori</i> by Solid‣tate NMR Spectroscopy. Angewandte Chemie - International Edition, 2016, 55, 14164-14168.	7.2	22
70	Solid-state NMR sequential assignment of the β-endorphin peptide in its amyloid form. Biomolecular NMR Assignments, 2016, 10, 259-268.	0.4	5
71	Solid-state NMR chemical-shift perturbations indicate domain reorientation of the DnaG primase in the primosome of Helicobacter pylori. Journal of Biomolecular NMR, 2016, 64, 189-195.	1.6	15
72	Sequence-specific solid-state NMR assignments of the mouse ASC PYRIN domain in its filament form. Biomolecular NMR Assignments, 2016, 10, 107-115.	0.4	12

5

#	Article	IF	CITATIONS
73	Solid-state NMR sequential assignments of the N-terminal domain of HpDnaB helicase. Biomolecular NMR Assignments, 2016, 10, 13-23.	0.4	16
74	Reassessment of MxiH subunit orientation and fold within native Shigella T3SS needles using surface labelling and solid-state NMR. Journal of Structural Biology, 2015, 192, 441-448.	1.3	18
75	Alternative salt bridge formation in Al̂²â€"a hallmark of early-onset Alzheimer's disease?. Frontiers in Molecular Biosciences, 2015, 2, 14.	1.6	17
76	Structure-based drug design identifies polythiophenes as antiprion compounds. Science Translational Medicine, 2015, 7, 299ra123.	5.8	130
77	Spinning proteins, the faster, the better?. Journal of Magnetic Resonance, 2015, 253, 71-79.	1.2	127
78	Structure and assembly of the mouse ASC inflammasome by combined NMR spectroscopy and cryo-electron microscopy. Proceedings of the National Academy of Sciences of the United States of America, 2015, 112, 13237-13242.	3.3	133
79	Protein resonance assignment at MAS frequencies approaching 100ÂkHz: a quantitative comparison of J-coupling and dipolar-coupling-based transfer methods. Journal of Biomolecular NMR, 2015, 63, 165-186.	1.6	91
80	Functional expression, purification, characterization, and membrane reconstitution of non-structural protein 2 from hepatitis C virus. Protein Expression and Purification, 2015, 116, 1-6.	0.6	15
81	The structure of fibrils from â€~misfolded' proteins. Current Opinion in Structural Biology, 2015, 30, 43-49.	2.6	61
82	Solid-state NMR sequential assignment of Osaka-mutant amyloid-beta (Aβ1â^'40 E22Δ) fibrils. Biomolecular NMR Assignments, 2015, 9, 7-14.	0.4	16
83	Atomicâ€Resolution Threeâ€Dimensional Structure of Amyloid β Fibrils Bearing the Osaka Mutation. Angewandte Chemie - International Edition, 2015, 54, 331-335.	7.2	245
84	Wheat germ cell-free expression: Two detergents with a low critical micelle concentration allow for production of soluble HCV membrane proteins. Protein Expression and Purification, 2015, 105, 39-46.	0.6	24
85	Unlike Twins: An NMR Comparison of Two α-Synuclein Polymorphs Featuring Different Toxicity. PLoS ONE, 2014, 9, e90659.	1.1	110
86	Solid-state NMR sequential assignments of the amyloid core of full-length Sup35p. Biomolecular NMR Assignments, 2014, 8, 349-356.	0.4	13
87	Solid-state NMR sequential assignments of the amyloid core of Sup35pNM. Biomolecular NMR Assignments, 2014, 8, 365-370.	0.4	6
88	Solid-state NMR sequential assignments of the C-terminal oligomerization domain of human C4b-binding protein. Biomolecular NMR Assignments, 2014, 8, 1-6.	0.4	1
89	Yet another polymorph of α-synuclein: solid-state sequential assignments. Biomolecular NMR Assignments, 2014, 8, 395-404.	0.4	42
90	Deâ€Novo 3D Structure Determination from Subâ€milligram Protein Samples by Solidâ€State 100â€kHz MAS NMR Spectroscopy. Angewandte Chemie - International Edition, 2014, 53, 12253-12256.	7.2	294

#	Article	IF	CITATIONS
91	Efficient and stable reconstitution of the ABC transporter BmrA for solid-state NMR studies. Frontiers in Molecular Biosciences, 2014, 1, 5.	1.6	25
92	Structural and functional characterization of two alpha-synuclein strains. Nature Communications, 2013, 4, 2575.	5.8	721
93	The Conformation of the Prion Domain of Sup35 p in Isolation and in the Fullâ€Length Protein. Angewandte Chemie - International Edition, 2013, 52, 12741-12744.	7.2	40
94	Automated solid-state NMR resonance assignment of protein microcrystals and amyloids. Journal of Biomolecular NMR, 2013, 56, 243-254.	1.6	39
95	PAIN with and without PAR: variants for third-spin assisted heteronuclear polarization transfer. Journal of Biomolecular NMR, 2013, 56, 365-377.	1.6	17
96	On the Behavior of Water at Subfreezing Temperatures in a Protein Crystal: Evidence of Higher Mobility Than in Bulk Water. Journal of Physical Chemistry B, 2013, 117, 11433-11447.	1.2	0
97	4D solid-state NMR for protein structure determination. Physical Chemistry Chemical Physics, 2012, 14, 5239.	1.3	42
98	A Sedimented Sample of a 59â€kDa Dodecameric Helicase Yields Highâ€Resolution Solidâ€State NMR Spectra. Angewandte Chemie - International Edition, 2012, 51, 7855-7858.	7.2	112
99	A Nativeâ€Like Conformation for the Câ€Terminal Domain of the Prion Ure2p within its Fibrillar Form. Angewandte Chemie - International Edition, 2012, 51, 7963-7966.	7.2	21
100	Properties of the DREAM scheme and its optimization for application to proteins. Journal of Biomolecular NMR, 2012, 53, 103-112.	1.6	23
101	Solid-state NMR sequential assignments of α-synuclein. Biomolecular NMR Assignments, 2012, 6, 51-55.	0.4	61
102	Probing Water Accessibility in HET-s(218–289) Amyloid Fibrils by Solid-State NMR. Journal of Molecular Biology, 2011, 405, 765-772.	2.0	33
103	Kinetic analysis of protein aggregation monitored by real-time 2D solid-state NMR spectroscopy. Journal of Biomolecular NMR, 2011, 49, 121-129.	1.6	6
104	Extensive de novo solid-state NMR assignments of the 33ÂkDa C-terminal domain of the Ure2 prion. Journal of Biomolecular NMR, 2011, 51, 235-243.	1.6	57
105	Wheat-germ cell-free production of prion proteins for solid-state NMR structural studies. New Biotechnology, 2011, 28, 232-238.	2.4	7
106	A Protonâ€Detected 4D Solidâ€State NMR Experiment for Protein Structure Determination. ChemPhysChem, 2011, 12, 915-918.	1.0	160
107	The Amyloid–Congo Red Interface at Atomic Resolution. Angewandte Chemie - International Edition, 2011, 50, 5956-5960.	7.2	132
108	Mechanism of Inhibition of Enveloped Virus Membrane Fusion by the Antiviral Drug Arbidol. PLoS ONE, 2011, 6, e15874.	1.1	106

Ανία ΒΑΫςκμανν

#	Article	IF	CITATIONS
109	Heteronuclear proton assisted recoupling. Journal of Chemical Physics, 2011, 134, 095101.	1.2	48
110	Protocols for the Sequential Solid‣tate NMR Spectroscopic Assignment of a Uniformly Labeled 25 kDa Protein: HETâ€s(1â€227). ChemBioChem, 2010, 11, 1543-1551.	1.3	126
111	Protein 3D structure determination by high-resolution solid-state NMR. Comptes Rendus Chimie, 2010, 13, 423-430.	0.2	11
112	Simultaneous use of solution, solid-state NMR and X-ray crystallography to study the conformational landscape of the Crh protein during oligomerization and crystallization. Advances and Applications in Bioinformatics and Chemistry, 2010, 3, 25.	1.6	0
113	NMR Structure and Ion Channel Activity of the p7 Protein from Hepatitis C Virus. Journal of Biological Chemistry, 2010, 285, 31446-31461.	1.6	119
114	Prions. Prion, 2010, 4, 72-79.	0.9	32
115	Atomic-Resolution Three-Dimensional Structure of HET-s(218â^289) Amyloid Fibrils by Solid-State NMR Spectroscopy. Journal of the American Chemical Society, 2010, 132, 13765-13775.	6.6	252
116	Characterization of different water pools in solid-state NMR protein samples. Journal of Biomolecular NMR, 2009, 45, 319-327.	1.6	239
117	The Molecular Organization of the Fungal Prion HET-s in Its Amyloid Form. Journal of Molecular Biology, 2009, 394, 119-127.	2.0	74
118	Prion Fibrils of Ure2p Assembled under Physiological Conditions Contain Highly Ordered, Natively Folded Modules. Journal of Molecular Biology, 2009, 394, 108-118.	2.0	68
119	Structural constraints for the Crh protein from solid-state NMR experiments. Journal of Biomolecular NMR, 2008, 40, 239-250.	1.6	22
120	Polarization Transfer over the Water–Protein Interface in Solids. Angewandte Chemie - International Edition, 2008, 47, 5851-5854.	7.2	44
121	3D Protein Structures by Solid‣tate NMR Spectroscopy: Ready for High Resolution. Angewandte Chemie - International Edition, 2008, 47, 6110-6113.	7.2	51
122	Methyl Proton Contacts Obtained Using Heteronuclear Through-Bond Transfers in Solid-State NMR Spectroscopy. Journal of the American Chemical Society, 2008, 130, 10625-10632.	6.6	19
123	Proton assisted recoupling and protein structure determination. Journal of Chemical Physics, 2008, 129, 245101.	1.2	183
124	3D Structure Determination of the Crh Protein from Highly Ambiguous Solid-State NMR Restraints. Journal of the American Chemical Society, 2008, 130, 3579-3589.	6.6	135
125	Characterization of Folding Intermediates of a Domain-Swapped Protein by Solid-State NMR Spectroscopy. Journal of the American Chemical Society, 2007, 129, 169-175.	6.6	15
126	Solid-State NMR Spectroscopy of a Paramagnetic Protein: Assignment and Study of Human Dimeric Oxidized Cull–ZnII Superoxide Dismutase (SOD). Angewandte Chemie - International Edition, 2007, 46, 1079-1082.	7.2	100

#	Article	IF	CITATIONS
127	High-resolution solid-state MAS NMR of proteins—Crh as an example. Magnetic Resonance in Chemistry, 2007, 45, S24-S31.	1.1	12
128	The influence of nitrogen-15 proton-driven spin diffusion on the measurement of nitrogen-15 longitudinal relaxation times. Journal of Magnetic Resonance, 2007, 184, 51-61.	1.2	57
129	Investigation of Dipolar-Mediated Waterâ~'Protein Interactions in Microcrystalline Crh by Solid-State NMR Spectroscopy. Journal of the American Chemical Society, 2006, 128, 8246-8255.	6.6	69
130	Observation of Heteronuclear Overhauser Effects Confirms the15Nâ^'1H Dipolar Relaxation Mechanism in a Crystalline Protein. Journal of the American Chemical Society, 2006, 128, 12398-12399.	6.6	36
131	Structural and dynamic studies of proteins by high-resolution solid-state NMR. Comptes Rendus Chimie, 2006, 9, 381-392.	0.2	26
132	Water–Protein Hydrogen Exchange in the Micro-Crystalline Protein Crh as Observed by Solid State NMR Spectroscopy. Journal of Biomolecular NMR, 2005, 32, 195-207.	1.6	50
133	Quantitative Analysis of Backbone Dynamics in a Crystalline Protein from Nitrogen-15 Spinâ^Lattice Relaxation. Journal of the American Chemical Society, 2005, 127, 18190-18201.	6.6	111
134	Proton to Carbon-13 INEPT in Solid-State NMR Spectroscopy. Journal of the American Chemical Society, 2005, 127, 17296-17302.	6.6	138
135	Site-Specific Backbone Dynamics from a Crystalline Protein by Solid-State NMR Spectroscopy. Journal of the American Chemical Society, 2004, 126, 11422-11423.	6.6	87
136	Probing Molecular Interfaces Using 2D Magic-Angle-Spinning NMR on Protein Mixtures with Different Uniform Labeling. Journal of the American Chemical Society, 2004, 126, 14746-14751.	6.6	87
137	Solid state NMR sequential resonance assignments and conformational analysis of the 2x10.4 kDa dimeric form of the Bacillus subtilis protein Crh. Journal of Biomolecular NMR, 2003, 27, 323-339.	1.6	158
138	Coherence transfer selectivity in two-dimensional solid-state NMR. Chemical Physics Letters, 2003, 376, 515-523.	1.2	2
139	Transverse Dephasing Optimized Solid-State NMR Spectroscopy. Journal of the American Chemical Society, 2003, 125, 13938-13939.	6.6	104
140	Resolution Enhancement in Multidimensional Solid-State NMR Spectroscopy of Proteins Using Spin-State Selection. Journal of the American Chemical Society, 2003, 125, 11816-11817.	6.6	66
141	Waterâ <sup>~,</sup> Protein Interactions in Microcrystalline Crh Measured by1Hâ <sup>~,</sup> 13C Solid-State NMR Spectroscopy. Journal of the American Chemical Society, 2003, 125, 13336-13337.	6.6	58
142	Dimerization of Crh by Reversible 3D Domain Swapping Induces Structural Adjustments to its Monomeric Homologue Hpr. Journal of Molecular Biology, 2003, 332, 767-776.	2.0	31
143	NMR Spectra of a Microcrystalline Protein at 30 kHz MAS. Journal of the American Chemical Society, 2003, 125, 15807-15810.	6.6	63
144	Partial NMR assignments for uniformly (13C, 15N)-enriched BPTI in the solid state. Journal of Biomolecular NMR, 2000, 16, 209-219.	1.6	232

#	Article	IF	CITATIONS
145	Involvement of Electrostatic Interactions in the Mechanism of Peptide Folding Induced by Sodium Dodecyl Sulfate Bindingâ€,‡. Biochemistry, 2000, 39, 8362-8373.	1.2	123
146	Characterization of the interaction between bovine pancreatic trypsin inhibitor and thiocyanate by NMR. Biophysical Chemistry, 1998, 71, 221-234.	1.5	11
147	Three-dimensional structure of the DNA-binding domain of the fructose repressor from Escherichia coli by 1H and 15N NMR. Journal of Molecular Biology, 1997, 270, 496-510.	2.0	40
148	Determination of fast proton exchange rates of biomolecules by NMR using water selective diffusion experiments. FEBS Letters, 1997, 418, 127-130.	1.3	24
149	Rapid estimation of relative amide proton exchange rates of 15 N-labelled proteins by a straightforward water selective NOESY-HSQC experiment. FEBS Letters, 1996, 383, 191-195.	1.3	19
150	Suppression of radiation damping during selective excitation of the water signal: The WANTED sequence. Journal of Biomolecular NMR, 1996, 8, 87-92.	1.6	34